Cosmological Nucleosynthesis in the Big-Bang and Supernovae

Toshitaka KAJINO[1,2,*]

[1]*National Astronomical Observatory, Mitaka, Tokyo 181-8588, Japan*

[2]*University of Tokyo, Graduate School of Science, Department of Astronomy, Bunkyo-ku, Tokyo 113-0033, Japan*

Recent observation of the power spectrum of Cosmic Microwave Background (CMB) Radiation has exhibited that the flat cosmology is most likely. This suggests too large universal baryon-density parameter $\Omega_b h^2 \approx 0.022 \sim 0.030$ to accept a theoretical prediction, $\Omega_b h^2 \leq 0.017$, in the homogeneous Big-Bang model for primordial nucleosynthesis. Theoretical upper limit arises from the sever constraints on the primordial ^{7}Li abundance. We propose two cosmological models in order to resolve the descrepancy; lepton asymmetric Big-Bang nucleosynthesis model, and baryon inhomogeneous Big-Bang nucleosynthesis model. In these cosmological models the nuclear processes are similar to those of the r-process nucleosynthesis in gravitational collapse supernova explosions.

Massive stars $\geq 10 M_\odot$ culminate their evolution by supernova explosions which are presumed to be the most viable candidate site for the r-process nucleosynthesis. Even in the nucleosynthesis of heavy elements, initial entropy and density at the surface of proto-neutron stars are so high that nuclear statistical equilibrium favors production of abundant light nuclei. In such explosive circumstances many neutron-rich radioactive nuclei of light-to-intermediate mass as well as heavy mass nuclei play the significant roles.

KEYWORDS: Big-Bang cosmology, supernovae, explosive nucleosynthesis

I. Big-Bang Cosmology

Recent progress in cosmological deep survey has clarified progressively the origin and distribution of matter and evolution of Galaxies in the Universe.

The origin of the light elements among them has been a topic of broad interest for its significance in constraining the dark matter component in the Universe and also in seeking for the cosmological model which best fits the recent data of cosmic microwave background (CMB) fluctuations. This paper is concerned with neutrinos during Big-Bang nucleosynthesis (BBN). In particular, we consider new insights into the possible role which degenerate neutrinos may have played in the early Universe[1)] .

There is no observational reason to insist that the universal lepton number is zero. It is possible, for example, for the individual lepton numbers to be large compared to the baryon number of the Universe, while the net total lepton number is small $L \sim B$. It has been proposed recently[2)] that models based upon the Affleck-Dine scenario of baryogenesis might generate naturally lepton number asymmetry which is seven to ten orders of magnitude larger than the baryon number asymmetry. Neutrinos with large lepton asymmetry and masses ~ 0.07 eV might even explain the existence of cosmic rays with energies in excess of the Greisen-Zatsepin-Kuzmin cutoff.[3)] It is, therefore, important for both particle physics and cosmology to carefully scrutinize the limits which cosmology places on the allowed range of both the lepton and baryon asymmetries.

1. Lepton Asymmetric Big-Bang Model

Although lepton asymmetric BBN has been studied in many papers[4)] (and references therein), there are several differences in the present work: For one , we have included finite temperature corrections to the mass of the electron and photon.[5)] Another is that we have calculated the neutrino annihilation rate in the cosmic comoving frame, in which the Møller velocity instead of the relative velocity is to be used for the integration of the collision term in the Boltzmann equations.[6,7)]

Neutrinos and anti-neutrinos drop out of thermal equilibrium with the background thermal plasma when the weak reaction rate becomes slower than the universal expansion rate. If the neutrinos decouple early, they are not heated as the particle degrees of freedom change. Hence, the ratio of the neutrino to photon temperatures, T_ν/T_γ, is reduced. The biggest drop in temperature for all three neutrino flavors occurs for $\xi_\nu \sim 10$. This corresponds to a decoupling temperature above the cosmic QCD phase transition. ξ_ν is the neutrino degeneracy parameter defined by $\xi_\nu = \mu_\nu/T_\nu$, where μ_ν is the chemical potential and T_ν is the neutrino temperature. Finite ξ_ν leads to a lepton asymmetric (L $\neq$ 0) Universe.

Non-zero lepton numbers affect nucleosynthesis in two ways. First, neutrino degeneracy increases the expansion rate. This increases the ^{4}He production. Secondly, the equilibrium n/p ratio is affected by the electron neutrino chemical potential, $\mathrm{n/p} = \exp\{-(\Delta M/T_{n\leftrightarrow p}) - \xi_{\nu_e}\}$, where ΔM is the neutron-proton mass difference and $T_{n\leftrightarrow p}$ is the freeze-out temperature for the relevant weak reactions. This effect either increases or decreases ^{4}He production, depending upon the sign of ξ_{ν_e}.

A third effect emphasized in this paper is that T_ν/T_γ can be reduced if the neutrinos decouple early. This lower temperature reduces the energy density of neutrinos during BBN, and slows the expansion of the Universe. This decreases ^{4}He production.

Figure 1 highlights the main result of this study, where we take $\xi_{\nu_\mu} = \xi_{\nu_\tau}$. For low $\Omega_{\rm b} h^2_{50}$ models, only the usual low values for ξ_{ν_e} and $\xi_{\nu_{\mu,\tau}}$ are allowed. Between $\Omega_{\rm b} h^2_{50} \approx 0.188$ and 0.3, however, more than one allowed region emerges. For $\Omega_{\rm b} h^2_{50} \gtrsim 0.4$ only the large degeneracy solution is allowed.

* Corresponding author, Tel. +81-422-34-3740, Fax. +81-422-34-3746, E-mail: kajino@nao.ac.jp

Neutrino degeneracy can even allow baryonic densities up to $\Omega_{\rm b}h^2_{50} = 1$.

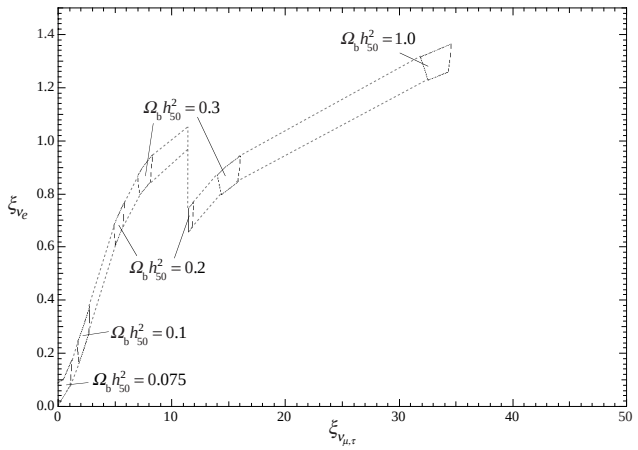

Fig. 1 Allowed values of ξ_{ν_e} and $\xi_{\nu_{\mu,\tau}}$ for which the constraints from light element abundances are satisfied for values of $\Omega_{\rm b}h^2_{50} = 0.075$, 0.1, 0.2, 0.3 and 1.0 as indicated. Note that $\Omega_{\rm b}h^2_{50} = 4 \times \Omega_{\rm b}h^2$, and $h = h_{100}$.

2. Cosmic Microwave Background

Several recent works[8–10] have shown that neutrino degeneracy can dramatically alter the power spectrum of the CMB. However, only small degeneracy parameters with the standard relic neutrino temperatures have been utilized. Here, we have calculated the CMB power spectrum to investigate effects of a diminished relic neutrino temperature.

The solid line on **Fig. 2** shows a $\Omega_\Lambda = 0.4$ model for which $n = 0.78$, where n is the power index of primordial fluctuations. This fit is marginally consistent with the data at a level of 5.2σ. The dotted line shows the matter dominated $\Omega_\Lambda = 0$ best fit model with $n = 0.83$ which is consistent with the data at the level of 3σ. The main differences in the fits between the large degeneracy models and our adopted benchmark model are that the first peak is shifted to slightly higher l value and the second peak is suppressed. One can clearly see that the suppression of the second acoustic peak is consistent with our derived neutrino-degenerate models. In particular, the MAXIMA-1 results are in very good agreement with the predictions of our neutrino-degenerate cosmological models. It is clear that these new data sets substantially improve the goodness of fit for the neutrino-degenerate models.[9] Moreover, both data sets seem to require an increase in the baryonic contribution to the closure density as allowed in our neutrino-degenerate models.[1,13]

3. Baryon Inhomogeneous Big-Bang Model

The biggest advantage of the baryon inhomogeneous Big-Bang nucleosynthesis model[14–16] is to allow larger $\Omega_{\rm b}h^2 \leq 0.05$, which well covers the constraint from recent CMB data $\Omega_b h^2 \approx 0.022 \sim 0.030$, still satisfying the light element abundance constraints.

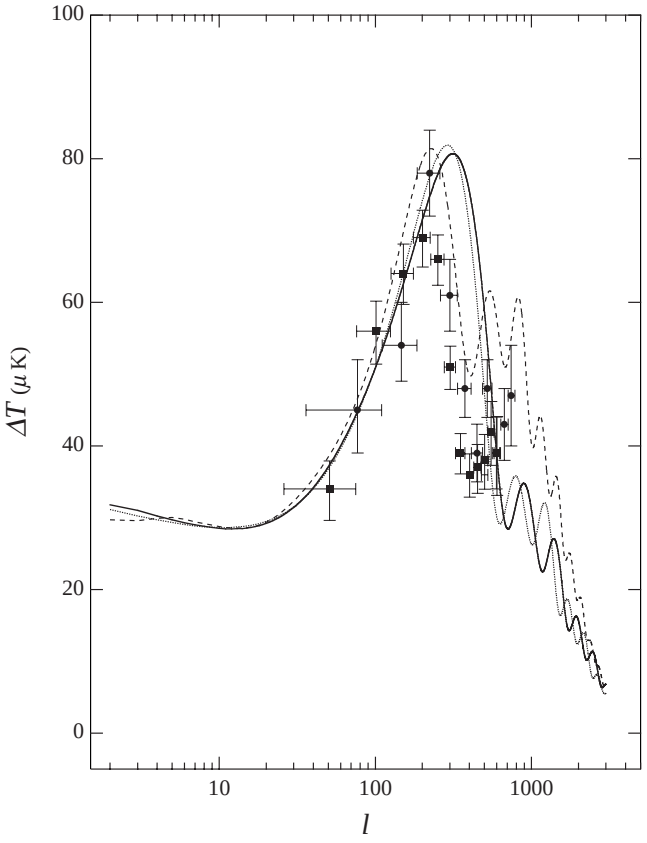

Fig. 2 CMB power spectrum from BOOMERANG[11] (squares) and MAXIMA-1[12] (circles) binned data compared with calculated $\Omega = 1$ models.

Let us consider what kind of observational signature is expected in this model. Nuclear reaction flow stops at the A = 7 nuclear systems in the homogeneous Big-Bang nucleosynthesis model because of the instability of ^{8}Be. In the baryon inhomogeneous model, however, the nucleosynthesis occurs in an environment of proton-neutron segregated inhomogeneous distribution. Therefore, the radioactive nuclear reactions play the significant roles in the production of intermediate-to-heavy mass elements via unstable nuclei ^{8}Li(838 ms), ^{9}Li(178.3 ms), ^{7}Be(53.29 d), ^{10}Be($1.51 \times 10^6 y$), ^{8}B(770 ms), ^{12}B(20.20 ms), ^{11}C(20.385 m), ^{14}C(5730 y), ^{15}C(2.449 s), ^{13}N(9.965 m), ^{16}N(7.13 s), ^{14}O(70.606 s), etc.

$$^4\mathrm{He}(^3\mathrm{H},\gamma)^7\mathrm{Li}(\mathrm{n},\gamma)^8\mathrm{Li}(\alpha,\mathrm{n})^{11}\mathrm{B}(\mathrm{n},\gamma)^{12}\mathrm{B}(\beta\,\nu) \quad (1)$$
$$^{12}\mathrm{C}(\mathrm{n},\gamma)^{13}\mathrm{C}(\mathrm{n},\gamma)^{14}\mathrm{C}...,$$

$$^7\mathrm{Li}(\mathrm{n},\gamma)^8\mathrm{Li}(\mathrm{n},\gamma)^9\mathrm{Li}(\beta\,\nu)^9\mathrm{Be}(\mathrm{n},\gamma)^{10}\mathrm{Be}(\mathrm{n},\gamma) \quad (2)$$
$$^{11}\mathrm{Be}(\beta\,\nu)^{11}\mathrm{B}...,$$

$$^7\mathrm{Li}(^3\mathrm{H},\mathrm{n})^9\mathrm{Be}(^3\mathrm{H},\mathrm{n})^{11}\mathrm{B}. \quad (3)$$

The two reaction chains (1) and (2) play the key roles in the production of heavy neutron-rich isotopes[14,16] in the neutron-rich zones. Since ^{7}Li is the heaviest element to be created

in the homogeneous Big-Bang nucleosynthesis model, all nuclear reactions for the production of heavier elements have ever been ignored in the previous calculations. We however found that the reaction chain (3) is extremely important for the production of ^{9}Be in the baryon inhomogeneous Big-Bang nucleosynthesis models.[17–19] With these reactions being included in the network of the baryon inhomogeneous Big-Bang models, the ^{9}Be abundance increases by three orders of magnitude to N(Be)/N(H) $\approx 10^{-14}$ which approaches the current observational level.

II. Supernova Explosion

Stars with various masses provide a variety of production sites for intermediate-to-heavy mass elements. Very massive stars $\geq 10M_\odot$ culminate their evolution by supernova (SN) explosions which are presumed to be most viable candidate for the still unknown astrophysical site of r-process nucleosynthesis. We discuss in this section the neutrino-driven winds from Type II SN explosion of very massive stars. Although there is still a room for the prompt explosion[20] to account for one part of the r-process nucleosynthesis, we concentrate on the gravitaional core-collpase Type II SNe here.

Even in the nucleosynthesis of heavy elements, initial entropy and density at the surface of proto-neutron stars are so high that nuclear statistical equilibrium (NSE) favors production of abundant light nuclei. In such explosive circumstances of so called hot-bubble scenario, not only heavy neutron rich nuclei but light unstable nuclei play a significant role.

The study of the origin of r-process elements is also critical in cosmology. It is a potentially serious problem that the cosmic age of the expanding Universe derived from cosmological parameters may be shorter than the age of the oldest globular clusters. Since both age estimates are subject to the uncertain cosmological distance scale, an independent method has long been needed. Thorium, which is a typical r-process element and has half-life of 14 Gyr, has recently been detected along with other elements in very metal-deficient stars. If we model the r-process nucleosynthesis in these first-generation stars, thorium can be used as a cosmochronometer completely independent of the uncertain cosmological distance scale.

1. Neutrino-Driven Winds in Type-II Supernovae

Recent measurements using high-dispersion spectrographs with large Telescopes or the Hubble Space Telescope have made it possible to detect minute amounts of heavy elements in faint metal-deficient ([Fe/H] $\leq$ -2) stars.[21] The discovery of r-process elements in these stars has shown that the relative abundance pattern for the mass region 120 $\leq$ A is surprisingly similar to the solar system r-process abundance independent of the metallicity of the star. Here metallicity is defined by [Fe/H] = log[N(Fe)/N(H)] - log[N(Fe)/N(H)]$_\odot$. It obeys the approximate relation t/10^{10}yr $\sim 10^{[Fe/H]}$. The observed similarity strongly suggests that the r-process occurs in a single environment which is independent of progenitor metallicity. Massive stars with $10M_\odot \leq M$ have a short life $\sim 10^7$ yr and eventually end up as violent supernova explosions, ejecting material into the intersteller medium early on quickly from the history of the Galaxy. However, the iron shell in SNe is excluded from being the r-process site because of the observed metallicity independence.

Hot neutron stars just born in the gravitational core collapse SNeII release most of their energy as neutrinos during the Kelvin-Helmholtz cooling phase. An intense flux of neutrinos heat the material near the neutron star surface and drive matter outflow (neutrino-driven winds). The entropy in these winds is so high that the NSE favors a plasma which consists of mainly free nucleons and alpha particles rather than composite nuclei like iron. The equilibrium lepton fraction, Y_e, is determined by a delicate balance between $\nu_e + n \rightarrow p + e^-$ and $\bar{\nu}_e + p \rightarrow n + e^+$, which overcomes the difference of chemical potential between n and p, to reach $Y_e \sim 0.45$. R-process nucleosynthesis occurs because there are plenty of free neutrons at high temperature. This is possible only if seed elements are produced in the correct neutron-to-seed ratio before and during the r-process.

Although Woosley et al.[22] demonstrated a profound possibility that the r-process could occur in these winds, several difficulties were subsequently identified. First, independent non relativistic numerical supernova models[23] have difficulty producing the required entropy in the bubble S/k $\sim$ 400. Relativistic effects may not be enough to increase the entropy dramatically.[24–26] Second, even should the entropy be high enough, the effects of neutrino absorption $\nu_e + n \rightarrow p + e^-$ and $\nu_e + A(Z,N) \rightarrow A(Z+1, N-1) + e^-$ may decrease the neutron fraction during the nucleosynthesis process. As a result, a deficiency of free neutrons could prohibit the r-process.[27]

In order to resolve these difficulties, we have studied[26, 28] neutrino-driven winds in a Schwarzschild geometry under the reasonable assumption of spherical steady-state flow. The parameters in the wind models are the mass of neutron star, M, and the neutrino luminosity, L_ν. The entropy per baryon, S/k, in the asymptotic regime and the expansion dynamic time scale, τ_{dyn}, which is defined as the duration time of the α-process when the temprature drops from T $\approx$ 0.5 MeV to 0.5/e MeV, are calculated from the solution of hydrodynamic equations. Then, we carried out r-process nucleosynthesis calculations in our wind model. We found[26] that the general relativistic effects make τ_{dyn} much shorter, although the entropy increases by about 40 % from the Newtonian value of S/k $\sim$ 90. By simulating many supernova explosions, we have found some interesting conditions which lead to successful r-process nucleosynthesis, as to be discussed in the following sections.

2. R-process Nucleosynthesis

Previous r-process calculations[22, 30] had complexity that the seed abundance distribution was first calculated by using smaller network for light-to-intermediate mass elements, and then the result was connected further to another r-process network in a different set of the computing run. For this reasaon it was less transparent to interpret the whole nucleosynthesis process. This inconvenience happened because it was numerically too heavy to run both α-process and r-process in a single network code for too huge number of reaction couplings among ~ 3000 isotopes. Our nucleosynthesis calculation[26, 28]

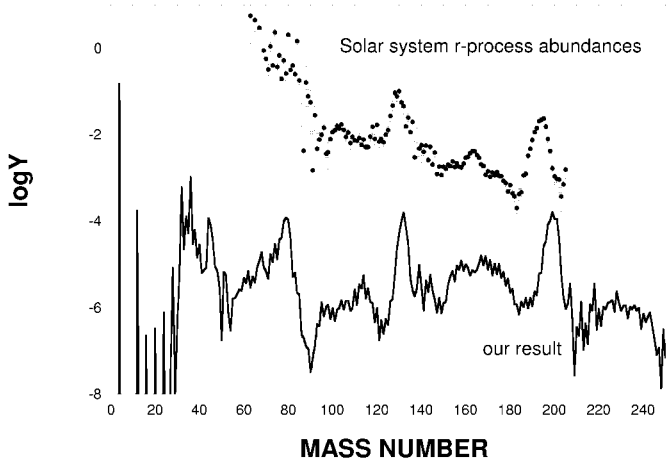

Fig. 3 R-process abundance[26] (solid line) as a function of atomic mass number A compared with the solar system r-process abundance (filled circles) from Käppeler, Beer, & Wisshak.[29] The neutrino-driven wind model used is for $L_\nu = 10^{52}$ ergs/s and $M = 2M_\odot$. The solar system r-process abundance is shown in arbitrary unit.

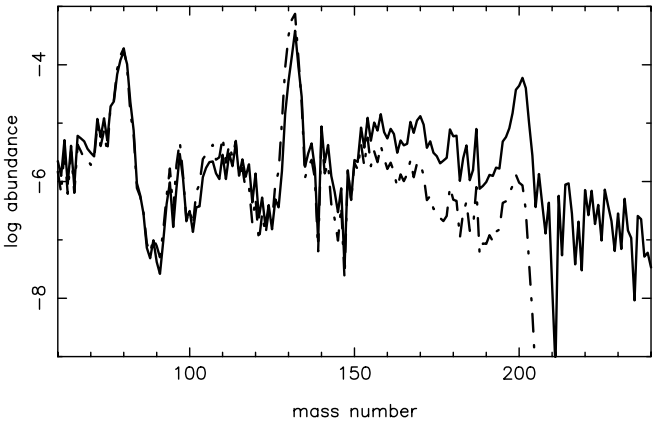

Fig. 4 The same as those in Figure 3, but for the neutrino-driven wind model of $L_\nu = 5 \times 10^{52}$ ergs/s. Solid line respresents the result by using the Woosley & Hoffman rate[31] of the ^{4}He$(\alpha n,\gamma)^9$Be reaction, and long-dashed line for the rate multiplied by factor 2, as suggested by the recent experiment of Utsunomiya et al.[32]

is completely free from this complexity because we exploited fully implicit single network code which is applied to a sequence of the whole processes of NSE - α-process - r-process.

Let us remind the readers that there were at least three difficulties in the previous theoretical studies of the r-process. The first difficulty among them is that an ideal, high entropy in the bubble S/k ~ 400[22] is hard to be achieved in the other simulations.[23–26]

The key to resolve this difficulty is found with the short dynamic time scale $\tau_{dyn} \sim 10$ ms in our models[26,28] of the neutrino-driven winds. As the initial nuclear composition of the relativistic plasma consists of neutrons and protons, the α-burning begins when the plasma temperature cools below T $\sim$ 0.5 MeV. The ^{4}He$(\alpha\alpha,\gamma)^{12}$C reaction is too slow at this temperature, and alternative nuclear reaction path ^{4}He$(\alpha n,\gamma)^9$Be$(\alpha,n)^{12}$C triggers explosive α-burning to produce seed elements with A ~ 100.[31] Therefore, the time scale for nuclear reactions is regulated by the ^{4}He$(\alpha n,\gamma)^9$Be. It is given by $\tau_N \equiv \left(\rho_b^2 Y_\alpha^2 Y_n \lambda(\alpha\alpha n \rightarrow {}^9\mathrm{Be})\right)^{-1}$. If the neutrino-driven winds fulfill the condition $\tau_{dyn} < \tau_N$, then fewer seed nuclei are produced during the α-process with plenty of free neutrons left over when the r-process begins at T $\sim$ 0.2 MeV. The high neutron-to-seed ratio, $n/s \sim 100$, leads to appreciable production of r-process elements, even for low entropy S/k ~ 130, producing both the 2nd $(A \sim 130)$ and 3rd $(A \sim 195)$ abundance peaks and the hill of rare-earth elements $(A \sim 165)$ **(Fig. 3)**.

The three body nuclear reaction cross section for ^{4}He$(\alpha n,\gamma)^9$Be is one of the poorly determined nuclear data which may alter the r-process nucleosynthesis yields. The inverse process has recently been studied experimentally by Utsunomiya et al.,[32] and photodisintegration cross section of ^{9}Be has been measured with better precision than those of the previous experiments. Applying the principle of the detailed balance to this process, one can estimate the cross section for ^{4}He$(\alpha n,\gamma)^9$Be. They found that the thermonuclear reaction rate is almost twice as big as that of Woosley and Hoffman[31] but in resonable agreement with recent compilation of Angulo et al.[33] However, there still remain several questions on the consistency between their result and electron-scattering experiments, on the contribution from the narrow resonance $J^\pi = 5/2^-$ (2.429 MeV), etc. It is also a theoretical challenge to understand the reaction mechanism and the resonance structure because two different channels, ^{8}Be + n and ^{5}He + α, contribute to this process.

Therefore, we show two calculated results in **Fig. 4**: The solid line displays the result obtained by using the Woosley and Hoffman cross section,[31] assuming a ^{8}Be + n structure for ^{9}Be. We also calculated the r-process by multiplying this cross section by factor of 2 (long-dashed line). This makes a drastic change in the r-process yields in the 3rd $(A \sim 195)$ abundance peak. More theoretical and experimental studies of the ^{4}He$(\alpha n,\gamma)^9$Be reaction are highly desired.

3. Neutrino-Nucleus Interactions

Neutrino interactions with nucleons and nuclei take the key to resolve the second difficulty which was pointed out in sect. 1. The difficulty is that the effects of neutrino absorptions $\nu_e + n \rightarrow p + e^-$ and $\nu_e + A(Z,N) \rightarrow A(Z+1,N-1) + e^-$ during the α-process may induce the deficiency of free neutrons and break down the r-process conditions.[27] These two types of neutrino interactions control most sensitively the electron fraction and the neutron fraction, as well, in a neutron-rich environment. In order to resolve this difficulty, we have updated the electron-type neutrino capture rates for all nuclei and electron-type anti-neutrino capture rate for free proton.[34,35]

The new r-process calculation proves to be almost invariant. One can understand this robustness of the succesful r-process in the following way: The specific collision time for neutrino-nucleus interactions is given by

$$\tau_\nu \approx 201 \times L_{\nu,51}^{-1} \times \left(\frac{\epsilon_\nu}{\mathrm{MeV}}\right)\left(\frac{r}{100\mathrm{km}}\right)^2\left(\frac{\langle\sigma_\nu\rangle}{10^{-41}\mathrm{cm}^2}\right)^{-1} ms, \quad (4)$$

where $L_{i,51}$ is the individual neutrino or antineutrino luminosity in units of 10^{51} ergs/s, $\epsilon_i =< E_i^2 > / < E_i >$ in MeV ($i = \nu_e,\ \bar{\nu}_e,\ etc.$), and $\langle\sigma_\nu\rangle$ is the averaged cross section over neutrino energy spectrum. At the α-burning site of r $\approx$ 100 km for $L_{\nu,51} \approx 10$, $\epsilon_{\nu_e} = 12$ MeV, and $\langle\sigma_\nu\rangle \approx 10^{-41} cm^2$, τ_{ν_e}(r=100 km) turns out to be ≈ 240 ms. This collision time is larger than the expansion dynamic time scale; $\tau_{dyn} \approx 10$ ms $\ll \tau_{\nu_e}$(r=100 km) ≈ 240 ms. Because there is not enough time for ν_e's to interact with n's in such rapidly expanding neutrino-driven wind, the neutron fraction is insensitive to the neutrino absorptions.

One might wonder if our dynamic time scale ~ 10 ms is too short for the wind to be heated by neutrinos. Careful comparison between proper expansion time and specific collision time for the neutrino heating is needed in order to answer this question. Otsuki et al.[26] have found that the supernova neutrinos transfer their kinetic energy to the wind most effectively just above the neutron star surface at $10\mathrm{km} \leq r < 20\mathrm{km}$. Therefore, one should refer the duration time for the wind to reach the α-burning site, τ_{heat}, rather than τ_{dyn}. One can estimate this heating time scale

$$\tau_{\mathrm{heat}} = \int_{r_i}^{r_f} \frac{dr}{u}, \quad (5)$$

where u is the fluid velocity of the wind. By setting the radius of neutron star surface $r_i = 10$ km and $r_f = 100$ km, we get $\tau_{\mathrm{heat}} \approx 30$ ms. The collision time τ_ν is given by Eq. (4) by setting $L_{\nu,51} \approx 10$, $\epsilon_\nu = (\epsilon_{\nu_e} + \epsilon_{\bar{\nu}_e})/2 = (12 + 22)/2 = 17$ MeV, r $\approx$10 km, and $\langle\sigma_\nu\rangle \approx 10^{-41} cm^2$. Let us compare τ_{heat} and τ_ν to one another: $\tau_\nu \approx 3.4\mathrm{ms} \ll \tau_{\mathrm{heat}} \approx 30\mathrm{ms}$. We can thus conclude that there is enough time for the expanding wind to be heated by neutrinos even with short dynamic time scale for the α-process, $\tau_{\mathrm{dyn}} \sim 10$ ms.

4. Roles of Light Neutron-Rich Nuclei

The r-process is thought to proceed after the pile up of seed nuclei produced in the α-process at higher temperatures $T_9 \approx 5 \sim 2.5$. Since charged-particle reactions, which reassemble nucleons into α-particles and α-particles into heavier nuclei (i.e. α-process), are faster than the neutron-capture flow which is regulated by beta-decays, the light-mass neutron-rich nuclei were presumed to be unimportant.

However, Terasawa et al.[36] have recently found that even light neutron-rich nuclei progressively play the significant roles in the production of seed nuclei. Nuclear reaction network used in the previous studies[22,30] includes only limited number of light unstable nuclei, ^{3}H, ^{7}Be, ^{8,9}B, ^{11,14}C, ^{13}N, ^{15}O, ^{18,20}F, ^{23,24}Ne, and so on. We therefore need to extend the network code so that it covers all radioactive nuclei to the neutron-drip line. We take the rates of charged particle reactions from those used in the Big-Bang nucleosynthesis calculations[16,18,19] and the NACRE compilation.[33]

Let us briefly discuss preliminary result of the r-process calculation, using the extended reaction network.[36] At early epoch of the wind expansion, t $\leq$ a few dozens ms, both temperature and density are so high that the charged particles interact with one aother to proceed nucleosynthesis around the β-stability line in the light-mass region A $\leq$ 20. There are plenty of protons and α-particles as well as neutrons at this epoch, and the main reaction flow is triggered by $^4\mathrm{He}(\alpha\mathrm{n},\gamma)^9\mathrm{Be}$:[22,31]

$$^4\mathrm{He}(\alpha\mathrm{n},\gamma)^9\mathrm{Be}(\alpha,\mathrm{n})^{12}\mathrm{C}(\mathrm{n},\gamma)^{13}\mathrm{C}(\alpha,\mathrm{n}) \quad (6)$$
$$^{16}\mathrm{O}(\mathrm{n},\gamma)^{17}\mathrm{O}(\alpha,\mathrm{n})^{20}\mathrm{Ne}\ \text{or}\ ^{16}\mathrm{O}(\alpha,\gamma)^{20}\mathrm{Ne}...$$

However, at relatively later epoch even after the α-rich freeze out, a new reaction path[36]

$$^3\mathrm{H}(\alpha,\gamma)^7\mathrm{Li}(\mathrm{n},\gamma)^8\mathrm{Li}(\alpha,\mathrm{n})^{11}\mathrm{B}(\mathrm{n},\gamma)^{12}\mathrm{B}(\mathrm{n},\gamma) \quad (7)$$
$$^{13}\mathrm{B}(\mathrm{n},\gamma)^{14}\mathrm{B}(\mathrm{n},\gamma)^{15}\mathrm{B}(\mathrm{e}^-\nu)^{15}\mathrm{C}...$$

also takes some appreciable flux of baryon number to continuously supply the seed nuclei. The classical r-process like flow, (n,γ) followed by beta decay, has already started from light nuclei. This is a very different result from the previous picture that the r-process starts from only intermediate-mass seed nuclei $A \approx 100$.

Since we do not have much information of $(2n,\gamma)$ reactions, we did not include ^{6}He, ^{8}He, ^{11}Li, ^{14}Be, ^{17,19}Be, ^{22}C, etc. The yields of even the most neutron-rich isotopes were found to be abundant in this calculation,[36] and we plan to study the possible role of the (2n,γ) reactions. There are several branching points between (n,γ) and (α,n) reactions. They are at ^{18}C, ^{24}O, ^{36}Mg, etc. Exerimetal studies to measure these reaction cross sections are highly desirable.

III. Quest for Nuclear Data and Astrophysics Data

Our result in Fig. 3 reproduces fairely well the observed second abundance peak (A $\approx$ 130), the hill of rare-earth elements (A $\approx$ 165), and the third peak (A $\approx$ 195). However, there are several defects, too. The first defect is a shift of the third abundance peak around A $\approx$ 195 by a couple of mass units. This is a common feature found in the previous r-process calculations,[22,26,30] too. These elements are the beta-decay products of extremely neutron-rich unstable nuclei on the neutron magic N = 126. Peak position depends on the timing of freezeout of the r-process. Therefore, a particular combination of environmental evolution of neutron-number density, N_n, and temperature, T_9, as well as the expansion dynamic time scale, τ_{dyn}, might match the freeze out so that it results in the right position of abundance peak.[36]

The second defect is the deficiency of abundance right above or below the peak elements, i.e. at A $\approx$ 90, 120, 150, 190, and 210. These deficiencies seem related to yet unseen effects of deformation or strucure change of unstable nuclei surrounding the neutron magic numbers N = 50, 82, and 126.

Further extensive theoretical studies and observational challenge to determine the masses, lives, and beta Q-values of these nuclei are highly desired.

The third defect is the underproduction of actinoid elements, Th-U-Pu (A = 230 $\sim$ 240), by more than one order of magnitude. The observed high abundance level of these nuclei might suggest an existence of a new magic number around N = 150 $\sim$ 160: Xenon $^{129}Xe_{75}$ and platinum $^{195}Pt_{117}$ are the typical r-process elements on the second and third abundance peaks, which are decay products from extremely neutron-rich unstable nuclei with neutron magic numbers N = 82 and 126, respectively. From these observations we estimate that the waiting point nucleus is located by shifting ΔN $\approx$ 7 or 9 units from the peak element. Applying the same shift ΔN $\approx$ 7 or 9 to $^{232}Th_{142}$ and $^{238}U_{146}$, we could assume a new magic number around N = 150 $\sim$ 160 which may lead to the fourth abundance peak at A = 230 $\sim$ 240. Actually, in the very light nuclear systems, a new magic number N = 16 was found[37] in careful experimental studies of the neutron separation energies and interaction cross sections of extremely neutron-rich nuclei. Since these possibilities were not taken into account in the present and previous calculations, the deficiency of actinoids might be improved by modernizing nuclear mass formula including such effects. Another possibility is to make actinoid elements in neutron star mergers or the mergers of the neutron star and black hole binaries which have extremely small lepton fraction, $Y_e \leq 0.2$.[38] However, these processes do not virtually produce any intermediate-mass nuclei including iron, which contradicts with the fact that the observed iron abundance is proportional to the r-process and actinoid elements over the entire history of Galactic evolution $\sim 10^{10}$ yr.

Since we discuss only material ejected from the proto-neutron star behind the shock, it does not make any serious problem to see the underproduction in mass region A $\leq$ 90. Most of these intermediat-mass nuclei are ejected from the exploded outer shells in supernovae.

Acknowledgment

This paper has been supported in part by the Grant-in-Aid for Science Researches 10044103, 10640236, 12047233 and 13640313 of the Ministry of Education, Science, Sports, and Culture of Japan.

References

1) M. Orito, T. Kajino, G. J. Mathews, R. N. Boyd, *Astrophys. J.*, submitted, (2000), astro-ph/0005446.
2) A. Casas, W. Y. Cheng, G. Gelmini, *Nucl. Phys. B.*, **538**, 297, (1999).
3) G. Gelmini, A. Kusenko *Phys. Rev. Lett.*, **82**, 5202, (1999).
4) H. Kang, G. Steigman *Nucl. Phys. B.*, **372**, 494, (1992).
5) N. Fornengo, C. W. Kim, J. Song, *Phys. Rev. D.*, **56**, 5123, (1997).
6) P. Gondolo, G. Gelmini, *Nucl. Phys. B.*, **360**, 145, (1991).
7) K. Enqvist, K, K. Kainulainen, V. Semikoz, *Nucl. Phys. B.*, **374**, 392, (1992).
8) W. K. Kinney, A. Riotto, *Phys. Rev. Lett.*, **83**, 3366, (1999).
9) J. Lesgourgues, S. Pastor, *Phys. Rev. D.*, **60**, 103521, (1999). astro-ph/0004412.
10) S. Hannestad, *Phys. Rev. Lett.*, submitted, (2000), astro-ph/0005018.
11) P. Bernardls, *et al.* (Boomerang Collaboration) *Nature.*, **404**, 955, (2000).
12) S. Hanany, *et al.* (MAXIMA-1 Collaboration), *Astrophys. J. Lett.*, submitted, (2000), astro-ph/0005123.
13) G. J. Mathews, M. Orito, T. Kajino, Y. Wang, *Phys. Rev. D.*, submitted, (2001).
14) J. H. Applegate, C. J. Hogan, R.J. Scherrer, *Phys. Rev. D.*, **35**, 1151, (1987).
15) C. R. Alcock, G. M. Fuller, G. J. Mathews, *Astrophys. J.*, **320**, 439, (1987).
16) T. Kajino, G.J. Mathews, G.M. Fuller, *Astrophys. J.*, **364**, 7, (1987).
17) R.N. Boyd, T. Kajino, *Astrophys. J. Lett.*, **336**, L55, (1989).
18) T. Kajino, R.N. Boyd, *Astrophys. J.*, **359**, 267, (1990).
19) M. Orito, T. Kajino, G. J. Mathews, *Astrophys. J.*, **488**, 515, (1997).
20) K. Sumiyoshi, M. Terasawa, G. J. Mathews, T. Kajino, S. Yamada, H. Suzuki, *Astrophys. J.*, **562**, 880, (2001).
21) C. Sneden, A. McWilliam, G. W. Preston, J. J. Cowan, D. L. Burris, B. J. Armosky, *Astrophys. J.*, **467**, 819, (1996).
22) S. E. Woosley, J. R. Wilson, G. J. Mathews, R. D. Hoffman, B. S. Meyer, *Astrophys. J.*, **433**, 229, (1994).
23) J. Witti, H.-Th. Janka, K. Takahashi, *Aatron. and Astrophys.*, **286**, 842, (1994).
24) Y. Z. Qian, S. E. Woosley, *Astrophys. J.*, **471**, 331, (1996).
25) C. Y. Cardall, G. M. Fuller, *Astrophys. J. Lett.*, **486**, L111, (1997).
26) K. Otsuki, H. Tagoshi, T. Kajino, S. Wanajo, *Astrophys. J.*, **533**, 424, (2000).
27) B. S. Meyer, *Astrophys. J. Lett.*, **449**, L55, (1995).
28) S. Wanajo, T. Kajino, G. J. Mathews, K. Otsuki, *Astrophys. J.*, **554**, 578, (2001).
29) F. Käppeler, H. Beer, K. Wisshak, *Rep. Prog. Phys.*, **52**, 945, (1989).
30) B. S. Meyer, G. J. Mathews, W. M. Howard, S. E. Woosley, R. D. Hoffman, *Astrophys. J.*, **399**, 656, (1992).
31) S. E. Woosley, R. D. Hoffman, *Astrophys. J.*, **395**, 202, (1992).
32) H. Utsunomiya, Y. Yonezawa, H. Akimune, T. Yamagata, M. Ohta, M. Fujishiro, H. Toyokawa, H. Ohgaki, *Phys. Rev. C.*, **63**, 018801, (2001).
33) C. Angulo *et al.* (NACRE collaboration), *Nucl. Phys. A.*, **656**, 3, (1999).
34) Y. -Z. Qian, W. C. Haxton, K. Langanke, P. Vogel, *Phys. Rev. C.*, **55**, 1533, (1997).
35) B. S. Meyer, G. C. McLaughlin, G. M. Fuller, *Phys. Rev. C.*, **58**, 3696, (1998).
36) M. Terasawa, K. Sumiyoshi, T. Kajino, G. J. Mathews, I. Tanihata, *Astrophys. J.*, **562**, 470, (2001).
37) A. Ozawa, T. Kobayashi, T. Suzuki, K. Yoshida, I. Tanihata, *Phys. Rev. Lett.*, **84**, 5493, (2000).
38) C. Freiburghaus, S. Rosswog, F.-K. Thielemann, *Astrophys. J. Lett.*, **525**, L121, (1999).